Journal of Molecular Structure 1226 (2021) 129360

Contents lists available at ScienceDirect

Journal of Molecular Structure

journal homepage: www.elsevier.com/locate/molstr

Ratiometric fluorescence imaging of Cu^{2+} based on spirolactamized benzothiazole-substituted *N,N*-diethylrhodol probe

Mengzhu Jin[a,b], Dandan Jin[a,b], Huawei Wang[a,b], Wenhao Yin[a,b,*]

[a] The First Hospital of Jiaxing, Jiaxing 314001, Zhejiang Province, China
[b] The Affiliated Hospital of Jiaxing University, Jiaxing 314001, Zhejiang Province, China

ARTICLE INFO

Article history:
Received 14 August 2020
Revised 26 September 2020
Accepted 27 September 2020
Available online 5 October 2020

Keywords:
N'*N*-diethylrhodol probe
Copper ion
Ratiometric fluorescence
Visual detection
Bioimaging

ABSTRACT

A novel ratiometric chemosensor **BSRH** based on spirolactamized benzothiazole-substituted *N,N*-diethylrhodol was developed for recognizing Cu^{2+}. In sensing process of **BSRH**, The Cu^{2+} was detected by the inhibition of ESIPT and formation of the delocalized xanthene with high sensitivity and selectivity. The Cu^{2+}-induced emission intensity/absorbance showed linearly proportional to the Cu^{2+}concentration (0.0–10.0 μM) with the low detection limit of 0.11 μM / 0.18 μM. Moreover, the probe was further successfully applied to test Cu^{2+} in real water samples and living Hela imaging. This work provides a promising and useful tool to determine Cu^{2+} in biological and environmental samples.

1. Introduction

Copper (Cu) was an essential transition metal element in the human body. [1,2] The lack of Cu^{2+} in human body may leads to Menke's disease, cardiovascular disease, Myelodysplastic syndrome et al. [3] Meanwhile, the excessive level of Cu^{2+} also results in some serious neurodegenerative diseases, including Alzheimer's diseases, Indian childhood cirrhosis, Wilson's diseases, Parkinson's diseases and cancer. [4,5] The WHO and EPA recommended safe limit intake of Cu^{2+} in the drinking water was approximately 1.3 ppm (20 μM). [7] In addition, Cu also played an indispensable role in many fundamental physiological processes in organisms. Recently, Cu^{2+} becomes a common metal pollutant in environment, due to the widespread use in industry and agriculture. [6] As a consequence, the monitoring and detection of Cu^{2+} in biological and environmental samples are of great significance.

Fluorescence sensing technique [8-11] had found widespread applications in the fluorescence imaging and detection of various target analytes in biological and environmental field owing to its prominent superiorities, such as easy operation, rapid response, low cost and high sensitivity. [12-15] Among various fluorescent probes, [16-20] ratiometric probes possessed more attractive advantages than turn-on / turn-off probes. The ratio of emission intensities at two different wavelengths could overcome the interference of external factors. [21-26] Therefore, developing of suitable ratiometric fluorescence probe to monitor the content of Cu^{2+} in environment and elucidate its distribution in physiological processes is of great importance for human health and environmental pollution. [27,28]

Herein, by grafting dihydroxyphenyl unit on benzoxazole appended xanthenes platform [29,30], a ratiometric probe **BSRH** was developed for tracking content changes of Cu^{2+} in the biological and environment systems (Scheme 1). The probe itself showed green fluorescence, which was attributed to the ESIPT of benzothiazole moiety. Upon the addition of Cu^{2+}, the bright green fluorescence significantly decreased and the red fluorescence brightened (the characteristic emission of opening-ring of rhodol spirolactam). More importantly, the further application of this probe for dynamic imaging of Cu^{2+} in biosystems has achieved.

2. Experimental

2.1. Materials and measurements

All chemicals were purchased from commercial suppliers and used without further purification. UV–Vis absorption and fluorescence spectra were performed on Shimadzu UV-1700 spectrophotometer and Hitachi F-4500 fluorescence spectrophotometer (ex-

* Corresponding author.
E-mail address: whyin69@sina.com (W. Yin).

https://doi.org/10.1016/j.molstruc.2020.129360
0022-2860/

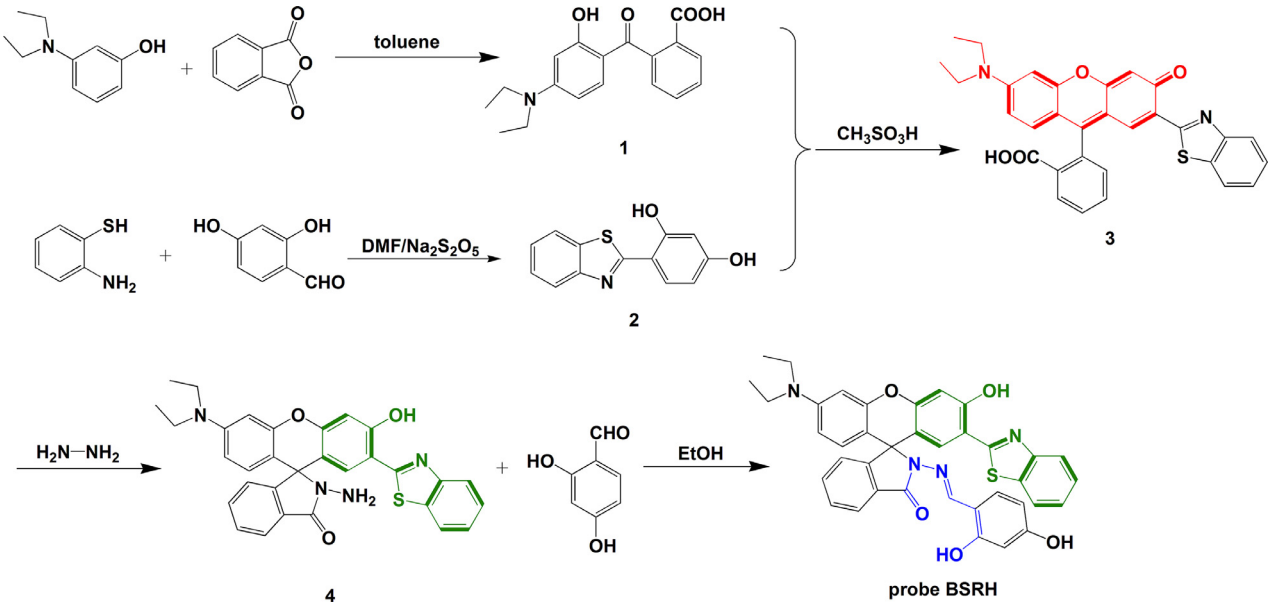

Scheme 1. Synthesis route of probe **BSRH**.

citation and emission slits set at 5.0 nm), respectively. High-resolution mass spectra (HR-MS) were measured by a Brukermicro TOF-QII ESI-Q-TOF LC/MS/MS Spectrometer. ^{1}H NMR and ^{13}C NMR spectra were recorded on a Varian INOVA-400 MHz spectrometer using tetramethylsilane as internal standard. The cell line Hela was obtained from Laboratory Center of the First Hospital of Jiaxing.

2.2. General procedure

The stock solution of probe **1** (1 mM) was prepared in MeOH. The solutions of $CuCl_2$ and other biologically relevant analytes stock solutions (1 mM) were prepared in deionized water. The hydrochloride salts of Zn^{2+}, Na^{+}, K^{+}, Ba^{2+}, Ca^{2+}, Cd^{2+}, Sn^{4+}, Mg^{2+}, Co^{2+}, Mn^{2+}, Pb^{2+}, Hg^{2+}, Ni^{2+}, Cr^{3+}, Al^{3+}, Fe^{2+}, Fe^{3+}, Cu^{2+} and the nitrate salt of Ag^{+} ions were used to evaluate the properties of the probe.

2.3. Synthesis of compound *3*

The compound **2** was prepared from 2-aminothiophenol and 2,4-dihydroxy- benzaldehyde . The compound **1** was prepared from 3-diethylaminophenol and *o*-phthalic anhydride according to the literature procedures. [31]

A suspension of **1** (0.243 g, 1 mmol) and **2** (0.313 g, 1 mmol) in methanesulfonic acid (20 mL) was stirred at 90 °C for 24 h. The reaction mixture was cooled to room temperature and then poured in ice-cold water (100 mL). The precipitate was filtered, washed with water (100 mL), and then dried under vacuum to give the crude product, which was further by column chromatography (CH_3OH / CH_2Cl_2 = 1 / 15) to afford compound **3** as a purple solid (0.256 g, yield: 49%). ^{1}H NMR(Chloroform-*d*, 400 MHz): δ (ppm) 1.22 (t, J = 7.0 Hz, 6H), 3.40 (q, J = 7.1 Hz, 4H), 5.32 (s, 1H), 6.33–6.71 (m, 3H), 6.95 (s, 1H), 7.07 (s, 1H), 7.29 (d, J = 3.0 Hz, 1H), 7.37 (t, J = 7.6 Hz, 1H), 7.47–7.51 (m, 1H), 7.67–7.74 (m, 2H), 7.80 (d, J = 7.9 Hz, 1H), 7.96 (d, J = 8.1 Hz, 1H), 8.10–8.13 (m, 1H). ^{13}C NMR(Chloroform-*d*, 100 MHz): δ (ppm) 12.5, 44.4, 65.4, 98.3, 104.8, 108.8, 114.1, 121.4, 121.9, 123.3, 123.8, 125.5, 126.7, 127.8, 128.7, 129.8, 132.3, 132.9, 150.9, 151.6, 153.3, 155.8, 159.1, 166.3, 168.3. MS (ESI) m/z = 521.1605 $[M + H]^{+}$, calc. for $C_{31}H_{25}N_2O_4S^{+}$ = 521.1530.

2.4. Synthesis of compound *4*

To a suspended solution of compound **3** (1 mmol, 0.52 g) in EtOH (30 mL) was added an excess of hydrazine monohydrate (51.5 mmol, 2.0 mL, 80%) and the solution was refluxed for 6 h. The resulting solution was evaporated in vacuum to give brownish black oil, which was further by column chromatography (CH_3OH / CH_2Cl_2 = 1 / 10) to afford compound **4** as a pale yellow solid (0.386 g, yield: 72%). ^{1}H NMR(Chloroform-*d*, 400 MHz): δ (ppm) 1.22 (t, J = 7.0 Hz, 6H), 3.38 (q, J = 7.1 Hz, 4H), 5.32 (s, 1H), 6.36 (dd, J = 8.9, 2.6 Hz, 1H), 6.47–6.50 (m, 2H), 6.94 (s, 1H), 6.98 (s, 1H), 7.15 (s, 1H), 7.18 (dd, J = 6.1, 2.5 Hz, 1H), 7.38 (t, J = 7.6 Hz, 1H), 7.48 (t, J = 7.7 Hz, 1H), 7.53–58 (m, 2H), 7.75 (s, 1H), 7.81 (d, J = 8.0 Hz, 1H), 7.93 (d, J = 8.2 Hz, 1H), 8.03 (dd, J = 6.3, 2.6 Hz, 1H). ^{13}C NMR(DMSO–d_6, 100 MHz): δ (ppm) 12.8, 29.4, 44.1, 85.6, 97.9, 103.0, 104.1, 105.0, 108.4, 109.4, 111.1, 112.3, 116.7, 122.2, 122.5, 123.7, 124.4, 125.2, 127.7, 129.6, 129.8, 131.9, 134.5, 135.0, 149.3, 150.7, 151.7, 152.6, 153.8, 154.7, 157.5, 159.9, 161.8, 163.3, 163.6. MS (ESI) m/z = 535.1798 $[M + H]^{+}$, calc. for $C_{31}H_{27}N_4O_4S^{+}$ = 535.1840.

2.5. Synthesis of probe ***BSRH***

Compound 4 (1 mmol, 0.534 g) and 2,4-Dihydroxybenzaldehyde (1.1 mmol, 0.152 g) were mixed in ethanol (25 mL) with addition of 2 drops of acetic acid. After refluxing for 24 h, the mixture was cooled to room temperature and evaporated to give deep yellow oil, which was further by column chromatography (CH_3OH / CH_2Cl_2 = 1 / 10) to afford probe **BSRH** as a pale yellow powder (0.457 g, yield: 70%). ^{1}H NMR(DMSO–d_6, 400 MHz): δ (ppm) 1.9 (t, J = 6.9 Hz, 6H), 3.35 (d, J = 7.0 Hz, 4H), 5.76 (s, 1H), 6.16 (d, J = 2.3 Hz, 1H), 6.25 (dd, J = 8.5, 2.2 Hz, 1H), 6.43–6.47 (m, 2H), 6.50 (d, J = 2.3 Hz, 1H), 6.97 (s, 1H), 7.16 (d, J = 8.5 Hz, 1H), 7.22–7.24 (m, 1H), 7.37 (d, J = 7.6 Hz, 1H), 7.43 (d, J = 7.8 Hz, 1H), 7.63 (s, 1H), 7.65–7.67 (m, 1H), 7.93 (d, J = 8.2 Hz, 1H), 7.99–8.01 (m, 1H), 8.04 (d, J = 7.9 Hz, 1H), 9.15 (s, 1H), 9.97 (s, 1H), 10.42 (s, 1H), 11.88 (s, 1H). ^{13}C NMR(DMSO–d_6, 100 MHz): δ (ppm) 12.8, 39.5, 44.1, 55.3, 65.6, 98.0, 103.7, 104.3, 109.5, 111.1, 117.1, 122.2, 122.6, 124.6, 125.3, 126.7, 126.9, 127.5, 128.0, 130.2, 135.2, 136.3, 142.8, 149.5, 151.6, 152.1, 154.1, 157.8, 162.9, 165.3, 192.4. MS (ESI) m/z = 655.2010 $[M + H]^{+}$, calc. for $C_{38}H_{31}N_4O_5S^{+}$ = 655.1942.

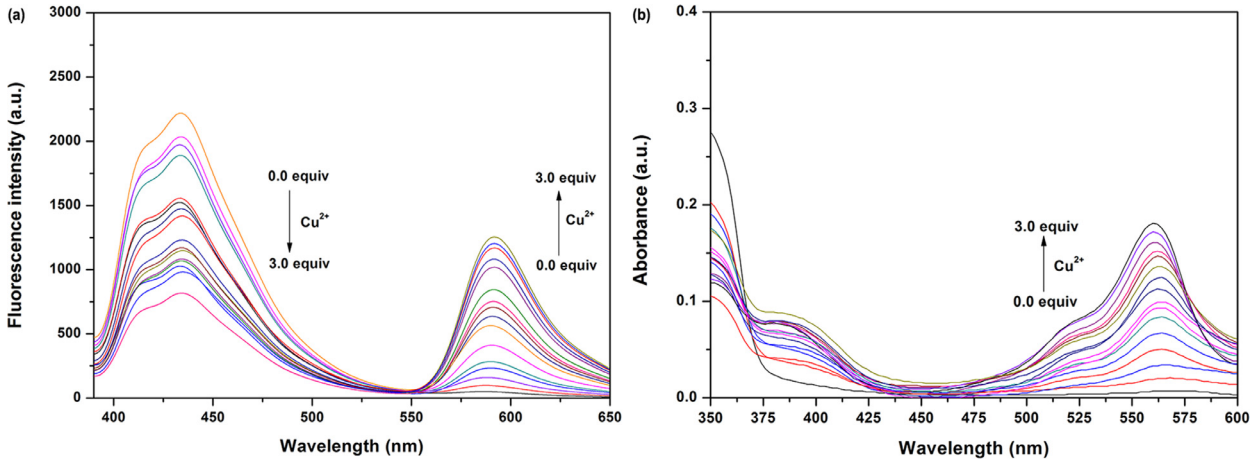

Fig. 1. Fluorescence spectra / UV–vis spectra of probe BSRH (10.0 μM) in the presence of the gradual addition of Cu^{2+}. λ_{ex} = 380 nm.

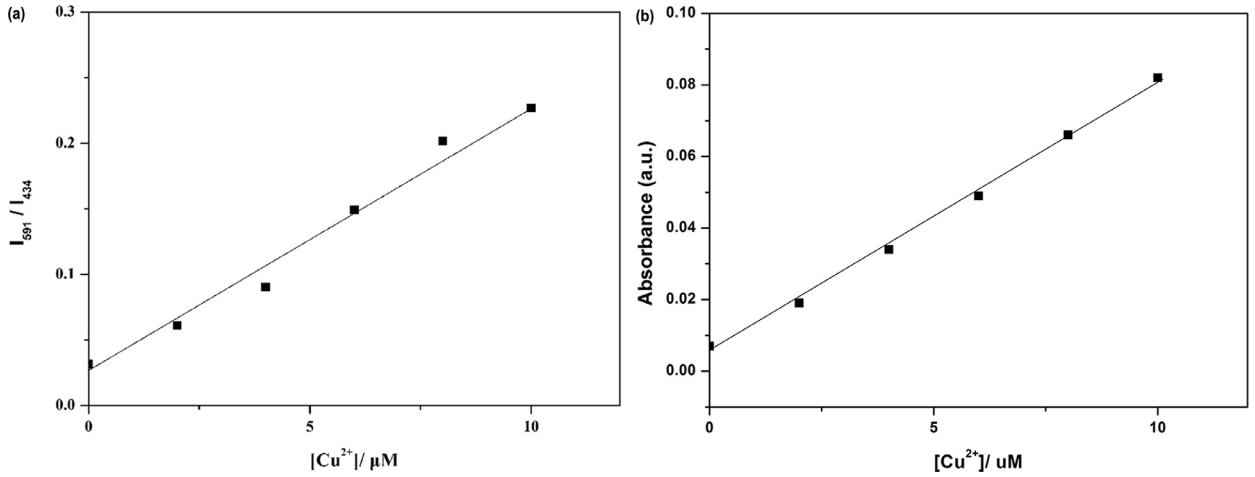

Fig. 2. A plot of the fluorescence intensity ratio (I_{591}/I_{434}) / absorbance (562 nm) versus Cu^{2+} (0.0–10.0 μM). λ_{ex} = 380 nm.

3. Results and discussion

3.1. Optical response towards Cu^{2+}

The signal response of probe **BSRH** towards $CuCl_2$ was recorded in MeOH-PBS (1/99, v/v, pH 7.4) solution in both fluorescence and UV–Vis spectra (Fig. 1). As expected, free probe **BSRH** showed a bright fluorescence at 434 nm corresponding to the formation of ESIPT effect. With the addition of Cu^{2+}, the emission band at 434 nm significantly decreased and the new emission band at 591 nm gradually enhanced, suggesting that Cu^{2+} induced the disappearance of the ESIPT effect and the opening of spirocylic ring of the xanthene moiety. Meanwhile, the visual color change from green to red under a 365 nm UV lamp for probe **BSRH** solution could be observed. The emission intensity ratio at 591 nm and 434 nm (I_{591}/I_{434}) of probe **BSRH** increased with the reaction time and reached a maximum with 20 min (Figure S1). Meanwhile, the emission intensity ratio (I_{591}/I_{434}) increased linearly as a function of the concentration of Cu^{2+} (0.0–10.0 μM). The regression equation was $y = 0.0306 \times [Cu^{2+}] + 0.102$ ($R^2 = 0.9831$) with the detection limit ($S/N = 3$) of 0.11 μM (Fig. 2). Similarly, probe **BSRH** exhibited a progressive increase in absorbance with the increasing of Cu^{2+} concentration (0.0–10.0 μM), as well as color changing from colorless to red by naked-eye for the **BSRH** probe solution. The regression equation was $y = 0.0054 \times [Cu^{2+}] - 0.0036$ ($R^2 = 0.986$) and the detection limit ($S/N = 3$) was calculated to be 0.18 μM. The results demonstrated that probe **BSRH** was a competent probe for the quantitative and qualitative detection of Cu^{2+}.

Subsequently, the changes in the fluorescence / absorption spectra of probe **BSRH** with different metal ions were evaluated (Fig. 3). Under the same testing conditions, there was not a noticeable change on the fluorescence intensity ratio / absorbance induced by other cations. The interference experiments were then conducted in the presence of Cu^{2+} (20.0 μM) and other competitive metal ions (100 μM). It was clearly shown that no appreciable changes in fluorescence / absorption behavior of probe **BSRH** for Cu^{2+} (20.0 μM) was observed by other interference metal ions (100 μM). The results suggested that probe **BSRH** could be used as an efficient probe for the detection of Cu^{2+}.

3.2. Proposed mechanism

To further ensure the binding site of the probe **BSRH**, the binding ratio between probe **BSRH** and Cu^{2+} was calculated based on the Job's plot analysis (Fig. 4). The maximum of fluorescence intensity ratio achieved when the molar fraction of Cu^{2+} was 0.5, indicating that complex ratio of **BSRH–Cu** was 1:1. Meanwhile, the association constant (Ka) of the probe **BSRH** on Cu^{2+} was calculated as $1.32 \times 10^5\ M^{-1}$.

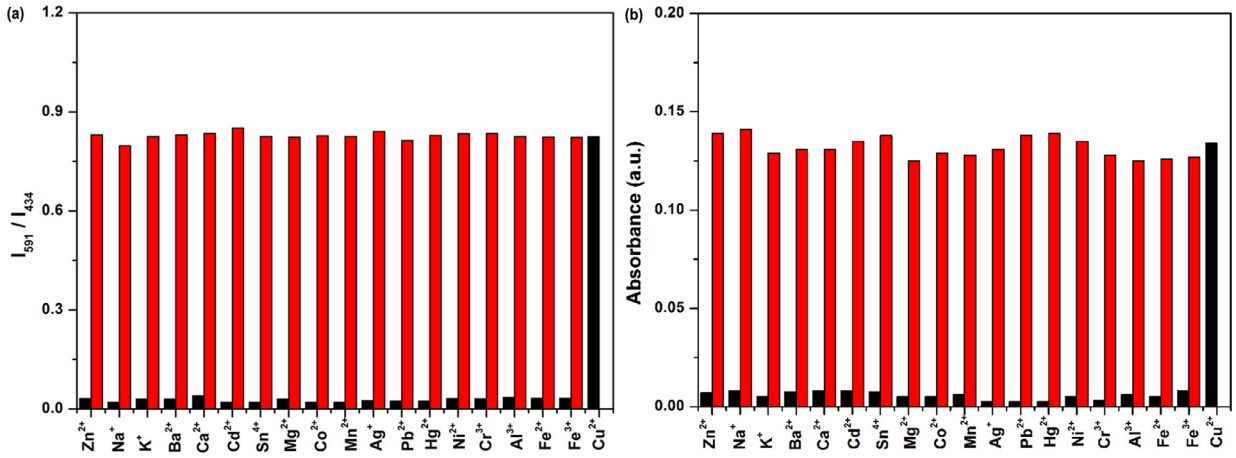

Fig. 3. (a) Fluorescence intensity ratio (I_{591}/I_{434}) of probe BSRH (10.00 μM, λ_{ex} = 380 nm) in MeOH-PBS (1/99, v/v, pH 7.4) solution and in the presence of different cations (100 μM) without (black) / with (red) Cu^{2+} (20.00 μM). (b) Absorbance of probe BSRH (10.00 μM) in the presence of different cations (100 μM) without (black) / with (red) Cu^{2+} (20.00 μM).

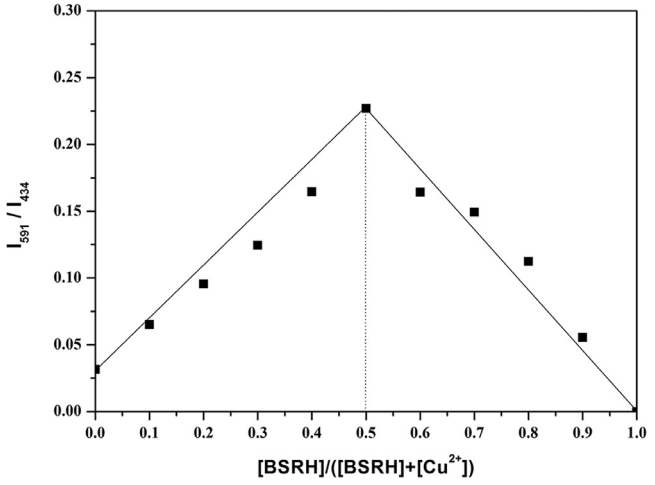

Fig. 4. Job's plot of probe **BSRH** and Cu^{2+}. The total concentration of probe **BSRH** and Cu^{2+} was 20 μM. λ_{ex} = 380 nm.

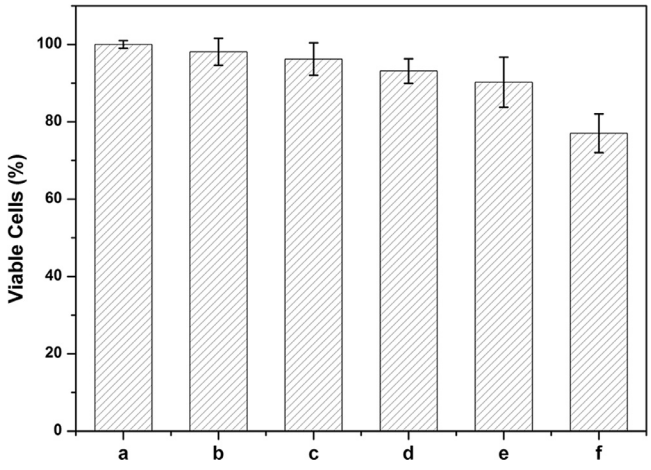

Fig. 5. MTT assay of Hela cells in the presence of different concentrations of probe **BSRH** (a: 0 μM; b: 0.1 μM; c: 1 μM; d: 10 μM; e: 100 μM; 1000 μM).

According to the fluorescence spectra results, the disappearance of the ESIPT effect and the opening of spirocylic ring of the delocalized xanthene had been established [32-33]. Thus, the proposed mechanistic pathway of the probe **BSRH** towards Cu^{2+} was deduced as follows (Scheme 2).

To strengthen the proposed mechanism, HRMS of probe **BSRH** by treated with Cu^{2+} was conducted. A major ion peak was obtained at *m/z* 716.1259 (Figure S11), which was characterized to be the ring opening product complex **BSRH + Cu** ($C_{38}H_{29}CuN_4O_5S$, calculated: *m/z* 716.1155). The results proved that probe BSRH directly interacted with Cu^{2+} to form a 1:1 complex.

3.3. Applications in real water samples

The practical application of the probe **BSRH** had been evaluated by the preliminarily determination of Cu^{2+} concentration in river water (Qiantang River) and tap water samples. The water samples were spiked with Cu^{2+} at different known concentrations, and the content of Cu^{2+} present in water sample was determined by measuring the ratio of emission intensity at 591 nm and 434 nm, respectively. As expected in Table 1, the analytical results obtained for these real samples showed good agreement with the Cu^{2+} spiked samples. The recoveries of the real water samples were in the range of 96.61- 103.29%, which were within an accept-

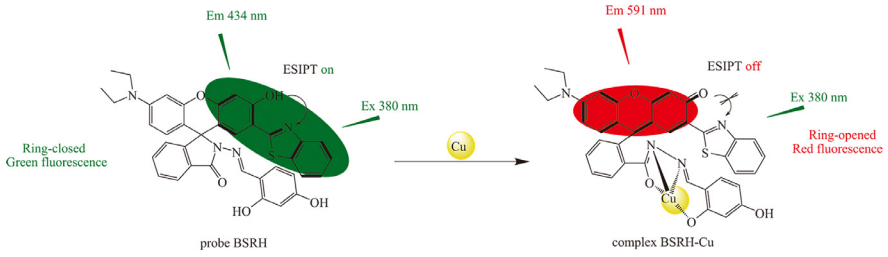

Scheme 2. Proposed response mechanism of probe BSRH.

Table 1
Application of the probe **BSRH** in real samples.

sample	Determined Cu^{2+} added (μM)	Spiked Cu^{2+} (μM)	Total found Cu^{2+} (μM)	Recovery (%)
tap	0.34 ± 0.02	3.00	3.45 ± 0.13	103.29
water		8.00	8.53 ± 0.27	102.28
River	0.53 ± 0.06	3.00	3.41 ± 0.17	96.61
water		8.00	8.58 ± 0.21	100.59

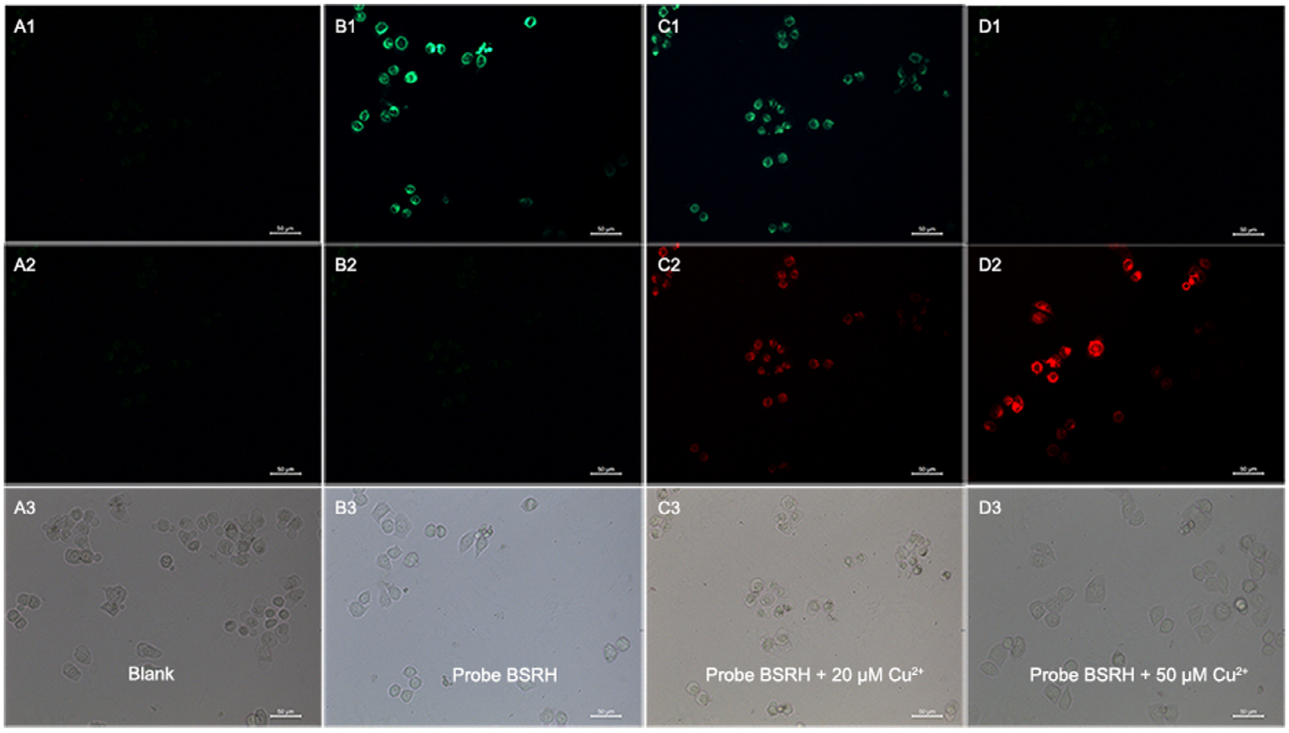

Fig. 6. Fluorescent images of Hela cells after incubation with probe BSRH (10.0 μM) in the absence and the presence of Cu^{2+}.

able range, suggesting that the components in real water samples did not cause serious interference in the detection of Cu^{2+}. Therefore, the proposed fluorescent probe had potential applications in the determination of Cu^{2+} in Cu^{2+}-contained water samples.

3.4. Visualization of Cu^{2+} in Hela cells

More importantly, we applied the **BSRH** probe for fluorescence imaging Cu^{2+} in Hela cells. Firstly, the toxicity of **BSRH** is evaluated by MTT assay result, displaying a low cytotoxicity in living Hela cells (Fig. 5). Then, the Hela cells which were pretreated with 10.0 μM probe **BSRH** displayed a strong green fluorescence (Fig. 6), suggesting that the probe was well membrane-permeable. When the cells were further supplemented with 20 μM Cu^{2+}, the bright green fluorescence significantly decreased and the red fluorescence brightened. After loading of 50 μM Cu^{2+} under the same condition, they exhibited intense red fluorescence but essentially no green fluorescence. These results established that the probe could be used to image Cu^{2+} in living cells.

4. Conclusions

In summary, we had successfully developed a novel ratiometric rhodol probe with a benzoxazole group. The probe exhibited colormetric and ratiometric fluorescence response to Cu^{2+} with high sensitivity and selectivity, through a unique spirocyclic ring-opening process. The Cu^{2+}-induced emission intensity/absorbance showed a good linear relationship with the concentration of Cu^{2+} in the range of 0.0 to 10.0 μM with a detection limit of 0.11 μM / 0.18 μM. Moreover, the probe was further employed to monitoring Cu^{2+} in real water samples and detection of exogenous Cu^{2+} in living cells, indicating its superb practical applications. This work provides a viewpoint for further design and synthesis of organic probe in biological and environmental samples.

Declaration of Competing Interest

The authors declare no competing financial interest.

CRediT authorship contribution statement

Mengzhu Jin: Writing - original draft, Methodology, Investigation. **Dandan Jin:** Methodology, Writing - original draft. **Huawei Wang:** Methodology, Data curation. **Wenhao Yin:** Supervision, Project administration, Writing - review & editing.

Acknowledgements

The work was supported by Zhejiang medical and health science and technology program (2019RC289), the Jiaxing Key Discipline of Chinese Medicine-Dermatology and Venereology of Integrative Medicine (Innovation) (No. 2019XK-C06).

Supplementary materials

Supplementary material associated with this article can be found, in the online version, at doi:10.1016/j.molstruc.2020.129360.

References

[1] D.W. Domaille, E.L. Que, C.J. Chang, Synthetic fluorescent sensors for studying the cell biology of metals, Nat. Chem. Biol. 4 (2008) 168–175, doi:10.1038/nchembio.69.

[2] S. Lutsenko, A. Gupta, J.L. Burkhead, V. Zuzel, Cellular multitasking: the dual role of human Cu-ATPases in cofactor delivery and intracellular copper balance, Arch. Biochem. Biophys. 476 (2008) 22–32, doi:10.1016/j.abb.2008.05.005.

[3] I. Bertini, A. Rosato, Menkes disease, Cell. Mol. Life Sci. 65 (2007) 89, doi:10.1007/s00018-007-7439-6.

[4] K.J. Barnham, C.L. Masters, A.I. Bush, Neurodegenerative diseases and oxidative stress, Nat. Rev. Drug Discov. 3 (2004) 205–214, doi:10.1038/nrd1330.

[5] D.J. Waggoner, T.B. Bartnikas, J.D. Gitlin, The Role of Copper in Neurodegenerative Disease, Neurobiol. Dis. 6 (1999) 221–230, doi:10.1006/nbdi.1999.0250.

[6] H. Zhang, X. Dong, J. Wang, R. Guan, D. Cao, Q. Chen, Fluorescence Emission of Polyethylenimine-Derived Polymer Dots and Its Application to Detect Copper and Hypochlorite Ions, ACS Appl. Mater. Inter. 11 (2019) 32489–32499, doi:10.1021/acsami.9b09545.

[7] S. Ishida, P. Andreux, C. Poitry-Yamate, J. Auwerx, D. Hanahan, Bioavailable copper modulates oxidative phosphorylation and growth of tumors, P. Natl. Acad. Sci. 110 (2013) 19507–19512, doi:10.1073/pnas.1318431110.

[8] L. Wang, M.S. Frei, A. Salim, K. Johnsson, Small-Molecule Fluorescent Probes for Live-Cell Super-Resolution Microscopy, J. Am. Chem. Soc. 141 (2019) 2770–2781, doi:10.1021/jacs.8b11134.

[9] D. Cao, Z. Liu, P. Verwilst, S. Koo, P. Jangjili, J.S. Kim, W. Lin, Coumarin-Based Small-Molecule Fluorescent Chemosensors, Chem. Rev. 119 (2019) 10403–10519, doi:10.1021/acs.chemrev.9b00145.

[10] X. Fang, Y. Zheng, Y. Duan, Y. Liu, W. Zhong, Recent Advances in Design of Fluorescence-Based Assays for High-Throughput Screening, Anal. Chem. 91 (2019) 482–504, doi:10.1021/acs.analchem.8b05303.

[11] S.-.H. Park, N. Kwon, J.-.H. Lee, J. Yoon, I. Shin, Synthetic ratiometric fluorescent probes for detection of ions, Chem. Soc. Rev. 49 (2020) 143–179, doi:10.1039/C9CS00243J.

[12] W. Chen, P. Xie, X. Shan, H. Zhao, Y. Wu, H. Zhou, X. Jin, A near-infrared naphthofluorescein-based fluorescent probe for hydrogen sulfide detection, J. Mol. Struct. 1207 (2020) 127822, doi:10.1016/j.molstruc.2020.127822.

[13] J. Xiong, Z. Li, J. Tan, S. Ji, J. Sun, X. Li, Y. Huo, Two new quinoline-based regenerable fluorescent probes with AIE characteristics for selective recognition of Cu2+ in aqueous solution and test strips, Analyst 143 (2018) 4870–4886, doi:10.1039/C8AN00940F.

[14] M. Tian, H. He, B.-.B. Wang, X. Wang, Y. Liu, F.-.L. Jiang, A reaction-based turn-on fluorescent sensor for the detection of Cu (II) with excellent sensitivity and selectivity: synthesis, DFT calculations, kinetics and application in real water samples, Dyes Pigments 165 (2019) 383–390, doi:10.1016/j.dyepig.2019.02.043.

[15] Y. Feng, Y. Yang, Y. Wang, F. Qiu, X. Song, X. Tang, G. Zhang, W. Liu, Dual-functional colorimetric fluorescent probe for sequential Cu2+ and S2− detection in bio-imaging, Sensor. Actuat. B-Chem. 288 (2019) 27–37, doi:10.1016/j.snb.2019.02.062.

[16] S. Zeng, S.-.J. Li, X.-.J. Sun, T.-.T. Liu, Z.-.Y. Xing, A dual-functional chemosensor for fluorescent on-off and ratiometric detection of Cu2+ and Hg2+ and its application in cell imaging, Dyes Pigments 170 (2019) 107642, doi:10.1016/j.dyepig.2019.107642.

[17] Y. Wang, H. Wu, W.-.N. Wu, X.-.J. Mao, X.-.L. Zhao, Z.-.Q. Xu, Z.-.H. Xu, Y.-.C. Fan, Novel rhodamine-based colorimetric and fluorescent sensor for the dual-channel detection of Cu2+ and Co2+/trivalent metal ions and its AIRE activities, Spectrochim. Acta A 212 (2019) 1–9, doi:10.1016/j.saa.2018.12.017.

[18] X. Jin, S. Zhao, T. Wang, L. Si, Y. Liu, C. Zhao, H. Zhou, X. Leng, X. Zhang, Near-infrared fluorescent probe for selective detection of H2S and its application in living animals, Anal. Bioanal. Chem. 411 (2019) 5985–5992, doi:10.1007/s00216-019-01973-1.

[19] Y. Cetinkaya, M.N.Z. Yurt, H. Avni Oktem, M.D. Yilmaz, A Monostyryl Boradiazaindacene (BODIPY)-based lanthanide-free colorimetric and fluorogenic probe for sequential sensing of copper (II) ions and dipicolinic acid as a biomarker of bacterial endospores, J. Hazard. Mater. 377 (2019) 299–304, doi:10.1016/j.jhazmat. 2019.05.108.

[20] M. Li, Z. Liu, S. Wang, D.G. Calatayud, W.-.H. Zhu, T.D. James, L. Wang, B. Mao, H.-.N. Xiao, Fluorescence detection and removal of copper from water using a biobased and biodegradable 2D soft material, Chem. Commun. 54 (2018) 184–187, doi:10.1039/C7CC08035B.

[21] P. Zhang, C. Fu, Q. Zhang, S. Li, C. Ding, Ratiometric Fluorescent Strategy for Localizing Alkaline Phosphatase Activity in Mitochondria Based on the ESIPT Process, Anal. Chem. 91 (2019) 12377–12383, doi:10.1021/acs.analchem.9b02917.

[22] W. Li, Z. Liu, B. Fang, M. Jin, Y. Tian, Two-photon fluorescent Zn2+ probe for ratiometric imaging and biosensing of Zn2+ in living cells and larval zebrafish, Biosens. Bioelectron. 148 (2020) 111666, doi:10.1016/j.bios.2019.111666.

[23] D. Zhu, X. Yan, A. Ren, W. Xie, Z. Duan, A novel colorimetric and ratiometric fluorescent probe for cysteine based on conjugate addition-cyclization-elimination strategy with a large Stokes shift and bioimaging in living cells, Anal. Chim. Acta 1058 (2019) 136–145, doi:10.1016/j.aca.2019.01.013.

[24] S. Yao, C. Ma, Y. Lu, X. Wei, X. Feng, P. Miao, G. Yang, J. Zhang, M. Yan, J. Yu, A FRET-based ratiometric two-photon fluorescent probe for superoxide anion detection and imaging in living cells and tissues, Analyst 144 (2019) 1704–1710, doi:10.1039/C8AN02196A.

[25] D. Pendin, R. Norante, A. De Nadai, G. Gherardi, N. Vajente, E. Basso, N. Kaludercic, C. Mammucari, C. Paradisi, T. Pozzan, A. Mattarei, A Synthetic Fluorescent Mitochondria-Targeted Sensor for Ratiometric Imaging of Calcium in Live Cells, Angew. Chem. Int. Edit. 58 (2019) 9917–9922, doi:10.1002/anie.201902272.

[26] Z. Chen, X. Mu, Z. Han, S. Yang, C. Zhang, Z. Guo, Y. Bai, W. He, An Optical/Photoacoustic Dual-Modality Probe: ratiometric in/ex Vivo Imaging for Stimulated H2S Upregulation in Mice, J. Am. Chem. Soc. 141 (2019) 17973–17977, doi:10.1021/jacs.9b09181.

[27] Y.-.H. Zhao, Y. Luo, H. Wang, H. Wei, T. Guo, H. Tan, L. Yuan, X.-.B. Zhang, A novel ratiometric and reversible fluorescence probe with a large Stokes shift for Cu2+ based on a new clamp-on unit, Anal. Chim. Acta 1065 (2019) 134–141, doi:10.1016/j.aca.2019.03.029.

[28] Y.M. Poronik, K.V. Vygranenko, D. Gryko, D.T. Gryko, Rhodols – synthesis, photophysical properties and applications as fluorescent probes, Chem. Soc. Rev. 48 (2019) 5242–5265, doi:10.1039/C9CS00166B.

[29] H. Wen, Q. Huang, X.-.F. Yang, H. Li, Spirolactamized benzothiazole-substituted N,N-diethylrhodol: a new platform to construct ratiometric fluorescent probes, Chem. Commun. 49 (2013) 4956–4958, doi:10.1039/C3CC41343H.

[30] M. Ren, B. Deng, K. Zhou, X. Kong, J.-.Y. Wang, G. Xu, W. Lin, A lysosome-targeted and ratiometric fluorescent probe for imaging exogenous and endogenous hypochlorous acid in living cells, J. Mater. Chem. B 4 (2016) 4739–4745, doi:10.1039/C6TB01085G.

[31] X. Jin, X. Wu, F. Zhang, H. Zhao, W. Zhong, Y. Cao, X. Ma, X. Leng, H. Zhou, M. She, Cu2+/ATP reversible ratiometric fluorescent probe through strip, hydrogel, and nanofiber, and its application in living cells and edaphic ecological safety assessment, Dyes Pigments 182 (2020) 108677, 10.1016/j.dyepig.2020.108677.

[32] P. Puangploy, S. Smanmoo, W. Surareungchai, A new rhodamine derivative-based chemosensor for highly selective and sensitive determination of Cu2, Sensor. Actuat. B-Chem. 193 (2014) 679–686, doi:10.1016/j.snb.2013.12.037.

[33] Y. Hu, J. Zhang, Y.-.Z. Lv, X.-.H. Huang, S.-l. Hu, A new rhodamine-based colorimetric chemosensor for naked-eye detection of Cu2 + in aqueous solution, Spectrochim. Acta A 157 (2016) 164–169, doi:10.1016/j.saa.2015.12.031.